

Delocalization in One-Dimensional Tight-Binding Models with Fractal Disorder II: Existence of Mobility Edge

Hiroaki S. Yamada¹

Yamada Physics Research Laboratory, Aoyama 5-7-14-205, Niigata 950-2002, Japan

Received: date / Revised version: date

Abstract. In the previous work, we investigated the correlation-induced localization-delocalization transition (LDT) of the wavefunction at band center ($E = 0$) in the one-dimensional tight-binding model with fractal disorder [Yamada, EPJB (2015) 88, 264]. In the present work, we study the energy ($E \neq 0$) dependence of the normalized localization length (NLL) and the delocalization of the wavefunction at the different energy in the same system. The mobility edges in the LDT arise when the fractal dimension of the potential landscape is larger than the critical value depending on the disorder strength, which is consistent with the previous result. In addition, we present the distribution of individual NLL and Lyapunov exponent in the system with LDT.

PACS. 72.15.Rn Localization effects – 72.20.Ee Mobility edges – 71.70.+h Metal-insulator transitions – 71.23.An Theories and models; localized states

1 Introduction

All eigenstates are exponentially localized in one-dimensional disordered systems (1DDS) with uncorrelated on-site disorder [1,2,3]. Recently, the study of delocalization phenomena in the 1DDS with long-range correlation have been performed using analytical as well as numerical methods [4,5,6,7,8,9,10,11,12,13]. In particular, many authors could numerically observe the correlation-induced localization-delocalization transition (LDT) in the 1D tight-binding model (TBM) by using the same potential sequences with power spectrum $S(f) \sim 1/f^\alpha$ ($\alpha \geq 2$) using Fourier filtering method (FFM), where f denotes frequency [11,12,14,15,16,17,18,19,20,21,22].

Very recently, Garcia and Cuevas modeled the sequences with the power-law spectrum by Weierstrass function with fractal dimension D and studied the transition based on the differentiability of the disorder potential as a necessary condition for the delocalization [23,24,25,26]. As a result, they could numerically demonstrate that the LDT takes place at the critical value $D_c = 3/2$ by means of the distribution of the energy level-spacing in the weak disorder limit.

In the previous paper [27], we have numerically reported that the finite-size scaling analysis for the normalized localization length (NLL) at the band center ($E = 0$) suggests the existence of the LDT around $D_c \simeq 3/2$ independent of the potential strength in the relatively weak disorder regime, as suggested by Garcia and Cuevas. On the other hand, in the relatively strong disorder regime, the critical fractal dimension D_c arrives at a smaller value than $3/2$ when varying the potential strength [27]. In ad-

dition, the existence of the power-law localized states has been observed in the case of relatively weak disorder strength for $D \geq 3/2$, which implies zero Lyapunov exponent. Such a power-law localization have been also observed in off-diagonal disordered systems and quantum percolation systems [30,31,32].

What remains a question is the delocalization of the other energy states of the TBM with the Weierstrass potential. In this study, therefore, we numerically investigate the delocalized behavior of the other energy states ($E \neq 0$) using the system size dependence of the NLL. We demonstrate the presence of the mobility edges and the power-law localized behavior for $D \gtrsim 3/2$ in the weak disorder cases. The critical value of D decreases with increasing the disorder strength W in the strong disorder regime.

On the other hand, the statistical properties of the individual NLL and Lyapunov exponent have not been studied in detail for the 1DDS with LDT, although the anomalous fluctuation might be expected [4,6]. With this in mind, we investigate here the statistical properties over ensemble and are able to verify the presence of the anomalous fluctuation, as well as to reveal the details of the system size dependence by taking large system size and large ensemble size as much as possible.

This paper is organized as follows. In the next section, we briefly introduce the 1DDS with the Weierstrass potential and some eigenstates. In Sect.3, we present global behavior of the E -dependence and N -dependence in the LDT by the numerical calculation of the NLL. In Sect.4, we present statistical distribution and convergence prop-

erty of the individual NLL and Lyapunov exponent with increasing the system size for the band edge state. Summary and discussion are presented in the last section.

2 Model

We consider the one-dimensional tight-binding Hamiltonian describing single-particle electronic states as

$$H = \sum_{n=1}^N V(n) C_n^\dagger C_n + \sum_{n=1}^{N-1} C_n^\dagger C_{n+1} + H.C., \quad (1)$$

where $C_n^\dagger (C_n)$ is the creation (annihilation) operator for the one-electron state at site n . The $\{V(n)\}_{n=0}^N$ and W are the disordered on-site energy sequence and the strength, respectively. The amplitude of the quantum state $|\Phi\rangle$ is given by $\phi(n) \equiv \langle \Phi | C_n^\dagger C_n | \Phi \rangle$ in the site representation. To model the correlated disorder potential for $V(n) (n \leq N)$ in Eq.(1), we use the following form:

$$V(n) = C \sum_{k=0}^L \frac{\sin(2\pi a^k n/N + \varphi_k)}{a^{(2-D)k}}, \quad (2)$$

where a is a constant value ($a > 1$) related the scale-invariance and D is a fractal dimension ($1 < D < 2$). $\{\varphi_k\}_{k=0}^L$ are random independent variables chosen in the interval $[0, 2\pi]$. C is the normalization constant which is determined by a condition

$$\sqrt{\langle V(n)^2 \rangle - \langle V(n) \rangle^2} = 1, \quad (3)$$

where $\langle \dots \rangle$ indicates the average over realization of the phases in Eq.(2). If we set $n/N = x$, $\varphi_k = 0$, the potential sequence becomes the "Weierstrass function" being continuous and indifferentiable everywhere by taking a continuous limit $N \rightarrow \infty$ and $L \rightarrow \infty$. Therefore, the potential will be shortly transferred to as "Weierstrass potential" in this paper, and we set $a = 2$ and $L = 50$ through this report without loss of the generality and accuracy of the numerical calculation. Figure 1 shows some potential landscapes. We can see that the landscape becomes smooth as the fractal dimension D decreasing. Note that the condition $\alpha \geq 2$ for the LDT corresponds to a condition $D \leq 3/2$ because the power spectrum $S(f)$ of the Weierstrass function is empirically characterized by $S(f) \sim \frac{1}{f^{5-2D}}$. The smoothness of the potential fluctuation can also induce the delocalization of the quantum states, which property is directly related to analyticity of the potential function in the continuum limit.

Garcia and Cuevas [23, 24] have numerically found that LDT at $D_c = 3/2$ for the sufficiently weak disorder regime by using the nearest-neighbor level-space distribution of the energy spectrum. It is useful to look at typical eigenstates directly to rationalize the effects of the fluctuation of the potential on the delocalization. Some typical eigenstates are shown in Fig.2. The state close to the band center as well as the one around band edge are localized

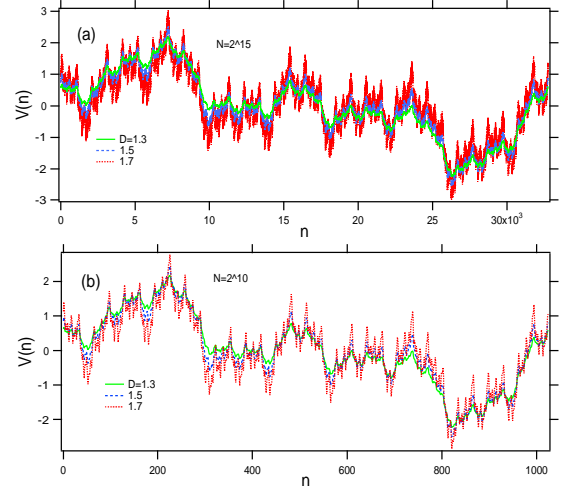


Fig. 1. (Color online) Typical on-site energy landscape $V(n)$ generated by the Eq.(2) and the normalization (3) with $D = 1.3, 1.5, 1.7$. (a) $N = 2^{15}$, (b) $N = 2^{10}$.

for $D = 1.7$, while the state near band center is delocalized for $D = 1.3$. These features are consistent with our previous work [27]. For small values of L some typical potential landscapes and the eigenstates are given in appendix A. In the next section, we investigate the energy dependence of the quantum states.

3 Numerical Results of the normalized localization length

We define the normalized localization length (NLL),

$$\Lambda_N \equiv \frac{\xi(N)}{N}, \quad (4)$$

where $\xi(N) (= \langle \gamma_N \rangle^{-1})$ denotes the finite size localization length (LL), and the finite size Lyapunov exponent $\gamma_N (N \gg 1)$ is defined by

$$\gamma_N = \frac{\ln(|\phi(N)|^2 + |\phi(N+1)|^2)}{2N}, \quad (5)$$

with the initial state $\phi(0) = \phi(1) = 1$. $\langle \dots \rangle$ denotes the ensemble average over different phases in Eq.(2). We numerically calculate the γ_N by using negative factor counting method [28, 29]. It is useful to study the LDT because Λ_N decreases (increases) with the system size N for localized (extended) states, and it becomes constant for the critical states.

In what follows, we investigate the NLL by changing the system size for some typical values of the system parameters, W , E . The typical size N and ensemble size used here are $N = 2^{14} \sim 2^{21}$ and $2^{11} \sim 2^{15}$, respectively. The robustness of the numerical calculations has been confirmed in each case.

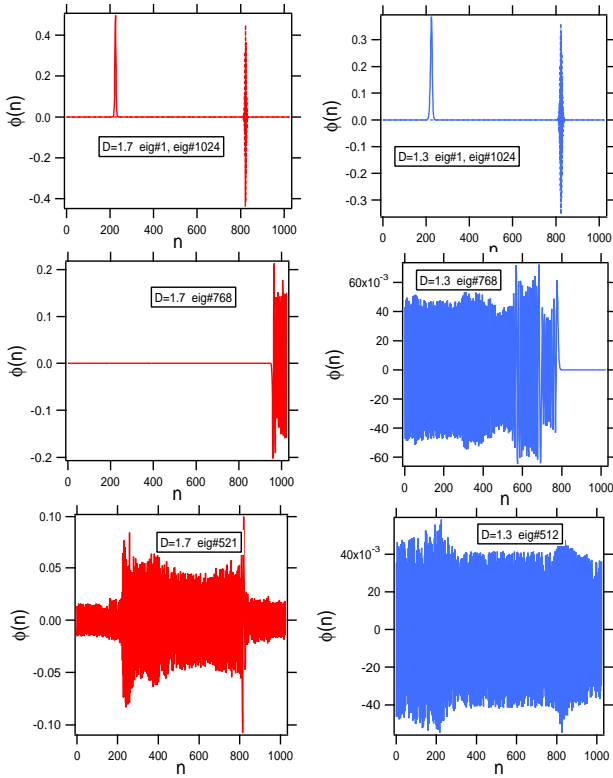


Fig. 2. (Color online) Comparison of some eigenstates $\{\phi(n)\}$ for the Weierstrasse potential in Fig.1(b) with $D = 1.7$ (left panels), $D = 1.3$ (right panels). $W = 0.75$, $N = 2^{10}$ and rigid boundary condition are used. The 1024th energy eigenstates (two top panels), 768th energy eigenstates (two middle panels), and the 512th energy eigenstates (two bottom panels) are shown from the top. The first energy eigenstates are also shown in two top panels. Note that the horizontal axis are in real scale.

3.1 Energy dependence:mobility edge

Figure 3 shows the energy dependence of the NLL for the different system sizes ($N = 2^{14} \sim 2^{21}$) with the fixed value $W = 0.5$. The E -dependence drops relatively smoothly down around $E \sim 0.7$ in the same way for all cases. In the case of $D = 1.7$, the NLL Λ_N goes to zero as $N \rightarrow \infty$ in all energy regime. In the cases of $D = 1.5$ and $D = 1.3$, the Λ_N arrives at the finite values greater than unity around the band center $|E| \lesssim 0.7$ as $N \rightarrow \infty$, while in the region outside of the center $|E| \gtrsim 0.7$, Λ_N decreases zero. Figure 4 shows detail of the E -dependence of the NLL around $E = 0.7$. It is apparent that the states get localized in the regime $|E| \gtrsim 0.7$. Λ_N exponentially decreases away from the edge $E \simeq 0.7$. The results suggest the existence of the mobility edge for $D \leq 3/2$ in the thermodynamic limit, which is consistent with the result by Garcia and Cuevas.

Furthermore, it was found that the LDT depends on the value of disorder strength W based on the result in Ref.[27]. Figure 5 shows the E -dependence of the Λ_N for some combinations of the disorder strength W and fractal dimension D at the fixed system size of $N = 2^{20}$. In the

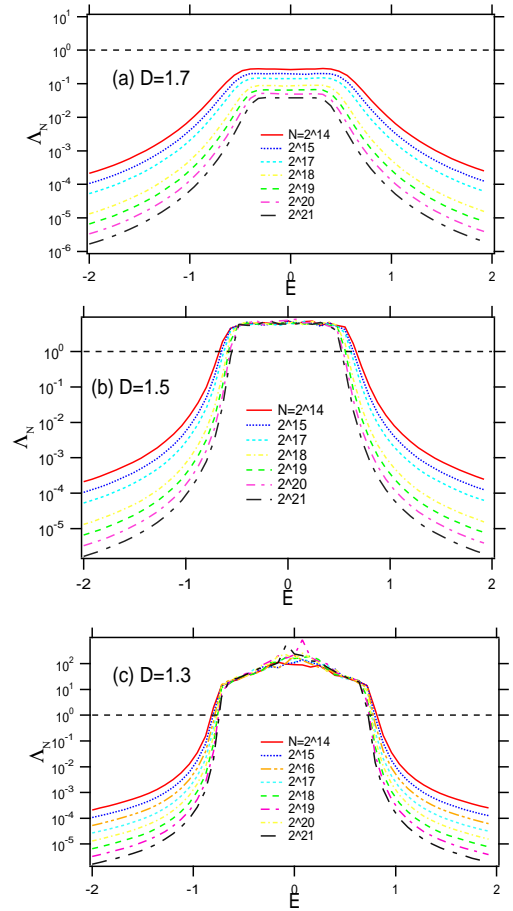


Fig. 3. (Color online) The normalized localization length Λ_N as a function of the energy E with a fixed value of $W = 0.5$ for $N = 2^{14} \sim 2^{21}$. (a) $D = 1.7$, (b) $D = 1.5$, (c) $D = 1.3$. Note that the data are plotted in logarithmic scale. The black broken lines denote $\Lambda_N = 1$ as a reference of LDT. The ensemble size is 2^{11} .

relatively strong disorder cases ($W \geq 0.5$), the delocalized states appear around the band center for $D \leq 3/2$. Figure 6 shows the detail of the E -dependence of Λ_N in the case of $W = 0.25$. In the relatively weak disorder case ($W = 0.25$), two peaks appear around $|E| \simeq 0.7$ when $D = 1.7$ although the states go to localized states with keeping the two-peaks structure of the E -dependence for $N \rightarrow \infty$, as shown in Fig.6(a). In the case of $D = 3/2$, the double-peaks structure of the E -dependence remains even for $N \rightarrow \infty$, as shown in Fig.6(b). The two peaks revealed ought to influence electronic transport and optical absorption.

3.2 system size dependence:power-law localization

Generally, the quantum states can be classified by the exponent δ of the N -dependence of the Λ_N when it behaves as,

$$\Lambda_N \sim N^\delta. \quad (6)$$

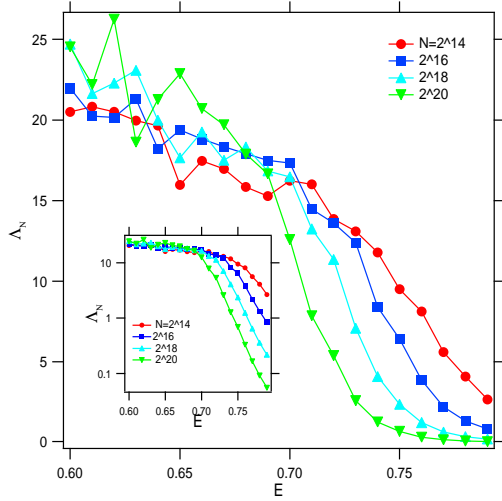


Fig. 4. (Color online) The normalized localization length Λ_N as a function of the energy E around $E \simeq 0.7$ of Fig.3(c) with $D = 1.3$ and $W = 0.5$. The ensemble size is 2^{12} . The inset shows the logarithmic plot.

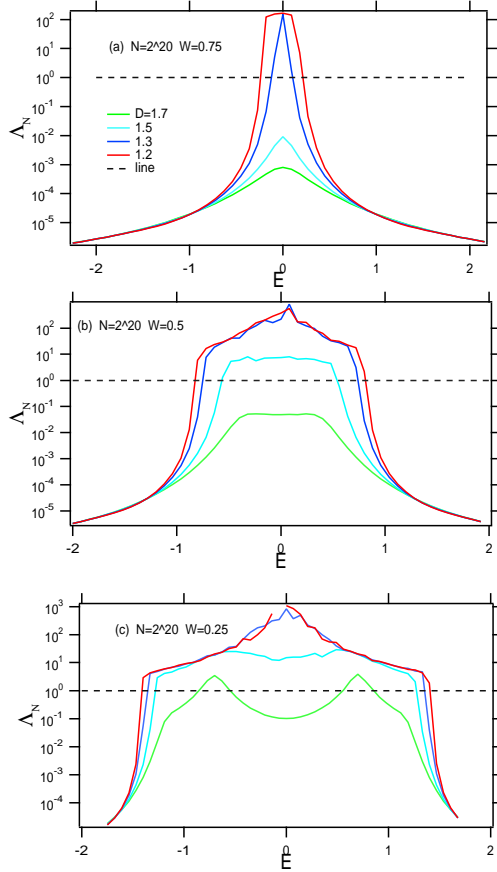


Fig. 5. (Color online) The normalized localization length Λ_N as a function of the energy E at $N = 2^{20}$ for $D = 1.2, 1.3, 1.5, 1.7$. (a) $W = 0.75$, (b) $W = 0.5$, (c) $W = 0.25$. Note that the data are plotted in logarithmic scale. The black broken lines denote $\Lambda_N = 1$ as a reference of LDT. The ensemble size is 2^{11} .

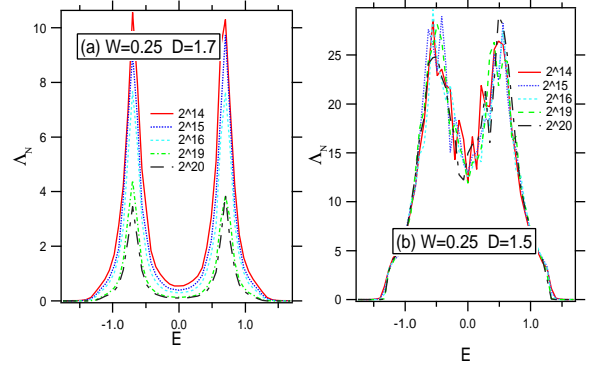


Fig. 6. (Color online) The normalized localization length Λ_N as a function of the energy E with a fixed value of $W = 0.25$ for $N = 2^{14} \sim 2^{19}$. (a) $D = 1.7$, (b) $D = 1.5$. Note that the data are plotted in real scales. The ensemble size is 2^{11} .

The exponent, $\delta \simeq 0$ for the extended states, $-1 < \delta < 0$ for the power-law localized states, and $\delta \simeq -1$ for the exponentially localized states. The states at the band center are more delocalized than the states away from the band center.

Figure 7(a) and (b) show the system size dependence of the NLL of a relatively strong disorder case ($W = 0.75$) in the vicinity of the band center and edge, respectively. It is found that the N -dependence changes the decreasing function with $\delta \simeq -1$ to the constant function $\delta = 0$ as the fractal dimension decreases in the case (a). It is found that the critical fractal dimension decreases with increasing the disorder strength, which is consistent with our previous result for $E \neq 0$. On the other hand, the states near band edge are exponentially localized irrespectively of the fractal dimension, as seen in Fig.7 (b).

Next, we have to pay attention to the delocalization of the states with energy away from $E = 0$ in the relatively weak disorder cases ($W \leq 0.5$), as given in Fig.7 (c) and (d). Note that the N -dependence of the NLL becomes independent of the system size for $D \leq 3/2$ in agreement with the extended nature of the states. The fact that the slopes of the straight lines in the log-log plot are $-1 < \delta < 0$ strongly suggests the power-law localization of the states. As a result it is suggested that the LDT takes place around the transition point $D_c = 3/2$ irrespectively of the disorder strength in relatively weak disorder regime $W \leq 0.5$, as shown in Ref.[27]. Exponential localization takes place for $D > 3/2$, while the behavior specific for the critical point arises in the whole range of $1 < D \leq D_c$. In the case of $W \ll 1$, the latter situation corresponds to the localization with the divergent localization length even for $D > 3/2$ and probably should be interpreted as the power-law localization.

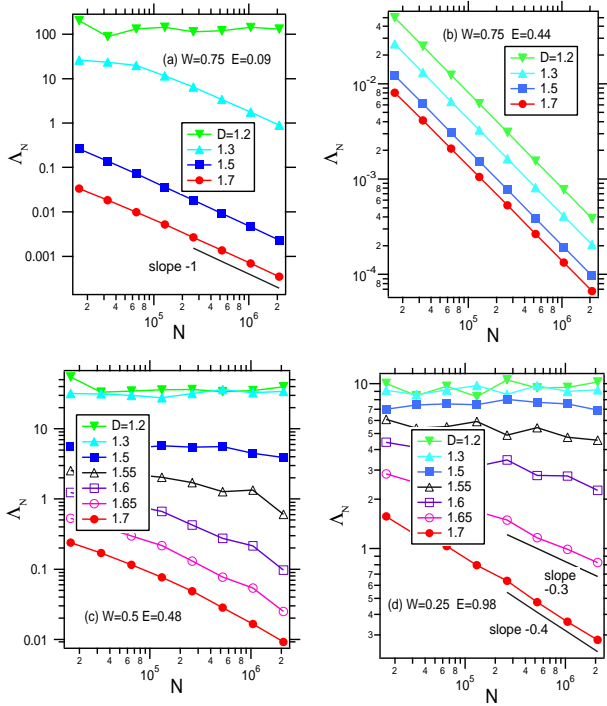


Fig. 7. (Color online) The normalized localization length Λ_N as a function of the system size N with several values of the fractal dimension. (a) $W = 0.75, E = 0.09$, (b) $W = 0.75, E = 0.44$ (c) $W = 0.5, E = 0.48$, (d) $W = 0.25, E = 0.98$. Note that the data plotted in double-logarithmic scale. The ensemble size is 2^{12} .

4 Distribution of individual normalized localization length and Lyapunov exponent

In this section, we discuss the statistical property of the distribution of individual NLL and Lyapunov exponent at $E = 1.0$ that is expected to correspond to a localized state.

First, we define the individual NLL $\Lambda_N^{(s)} \equiv 1/(N\gamma_N^{(s)})$, where $\gamma_N^{(s)}$ is Lyapunov exponent of a finite system with system size N and the suffix s run for each sample. Note that the mean value $\langle \Lambda_N^{(s)} \rangle$ satisfies inequality $\Lambda_N < \langle \Lambda_N^{(s)} \rangle$ because $\langle \gamma_N \rangle > 1/\langle 1/\gamma_N \rangle$. Figure 8 shows the histograms of the distribution of $\Lambda_N^{(s)}$ around band edge ($E = 1.0$) over 2^{15} samples. In the case of $D = 1.6$, the asymptotic behavior of the distribution of $\Lambda_N^{(s)}$ gradually moves to the origin position with increasing system size N . On the other hand, it is found that in the case of $D = 1.5$, it converges the distribution form with power-law tail. The N -dependence of the mean value $\langle \Lambda_N^{(s)} \rangle$ and the standard deviation σ_Λ are shown in Fig.9. The N -dependence is unstable and a clear difference does not appear between the cases of $D = 1.6$ and $D = 1.5$, different from cases of Λ_N in the last section.

In localized regime such as $D = 1.6$ and $D = 1.5$ around the band edge, Lyapunov exponent γ_N is better than $\Lambda_N^{(s)}$ to study the localization property. Fig.10 shows the histogram of the distribution of Lyapunov exponents

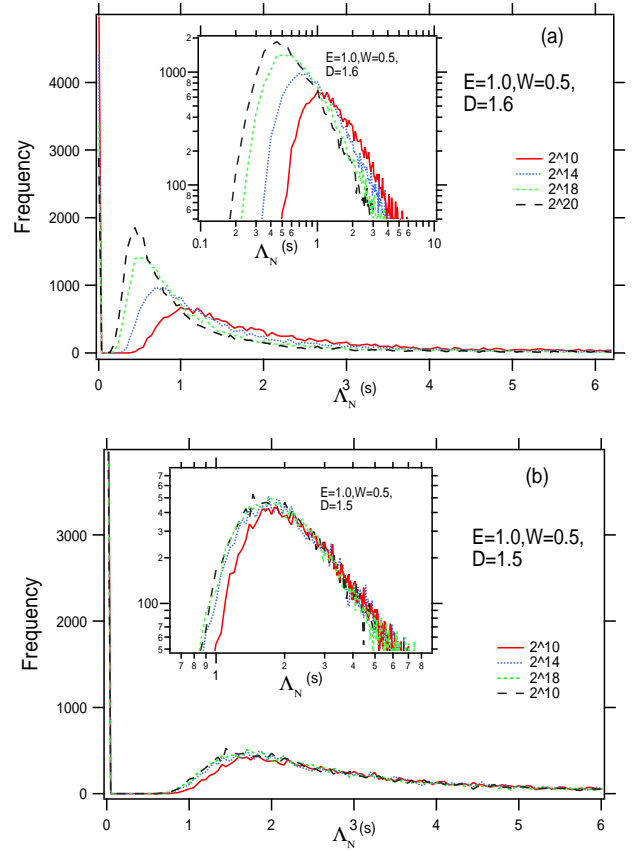


Fig. 8. (Color online) Histograms of the distribution of $\Lambda_N^{(s)}$ around band edge over 2^{15} samples in the cases (a) $D = 1.6$ and (b) $D = 1.5$. The other parameters are $W = 0.5, E = 1.0$. The details behavior around $\Lambda_N^{(s)} \sim 0$ is shown in each inset in the log-log plot. and the mesh of the horizontal line is 5×10^{-2} .

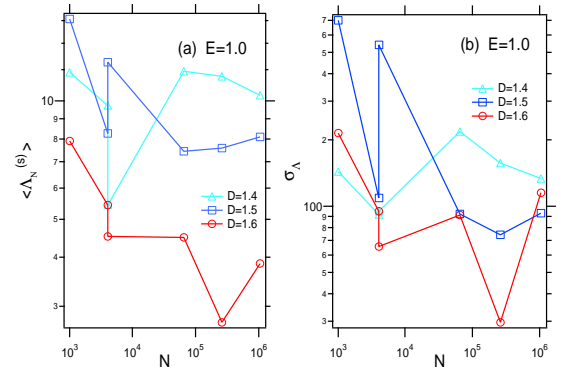


Fig. 9. (Color online) Log-log plot of (a) mean $\langle \Lambda_N^{(s)} \rangle$ and (b) standard deviation σ_Λ of the distribution in Fig.8 as a function of system size N at $E = 1.0$ for fractal dimension $D = 1.4, 1.5, 1.6$.

around band edge ($E = 1.0$) over 2^{15} samples. As a result the two kinds of distribution coexist. One of the two peaks around $\gamma_N \simeq 0$ corresponds to the extended states or power-law localized states. Fig.11 shows N -dependence of the mean value $\langle \gamma_N \rangle$ and standard deviation σ_{γ_N} of the distribution for some cases. We estimate the Lyapunov exponent γ_∞ for $N \rightarrow \infty$ by fitting the relation,

$$\langle \gamma_N \rangle = c_1 N^{-\alpha} + \gamma_\infty, \quad (7)$$

for all the cases in Fig.11(a). The estimated parameters are shown in Fig.12. As a result, at least, the Lyapunov exponent becomes zero, $\gamma_\infty \simeq 0$, for $D \leq 1.7$ at the band edge ($E = 1.0$), which is consistent with power-law localization in the last section.

The distribution form tends to be anomalous around the LDT and the ensemble-averaged value of the finite system size becomes unstable. Accordingly, it is important to investigate the statistical property of the distribution around the transition point because it is sensitive to the difference of the definition, as seen in this section.

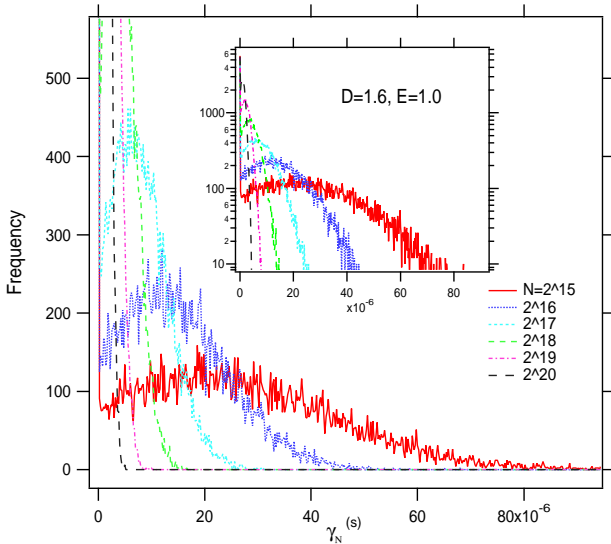


Fig. 10. (Color online) Histograms of the distribution of γ_N around band edge ($E = 1.0$) in the case of $D = 1.6$. The details behavior around $\gamma_N \sim 0$ is shown in the inset in the semi-log plot. The ensemble size is 2^{15} and the mesh of the horizontal line is 2×10^{-7} .

5 Summary and discussion

In summary, we have numerically studied the nature of LDT in 1DDS with fractal disorder generated by Weierstrass function. We have explicitly shown some basic features of the system. We used the normalized localization length defined by the Lyapunov exponent to investigate the delocalized behavior of the wavefunctions for the entire energy region. The results suggest that in the weak disorder cases

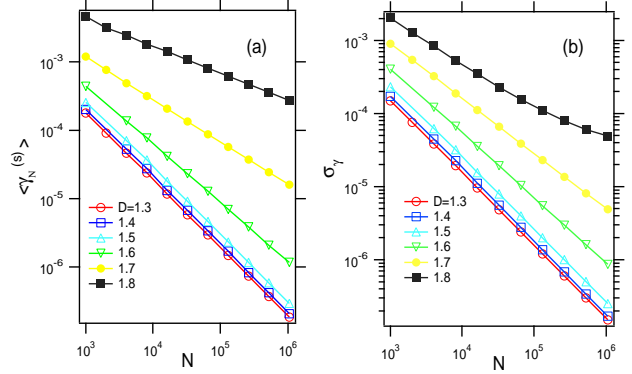


Fig. 11. (Color online) Log-log plot of (a) mean $\langle \gamma_N \rangle$ and (b) standard deviation σ_{γ} of the distribution in Fig.8 as a function of system size N at $E = 1.0$ for fractal dimension $D = 1.4, 1.5, 1.6$. A relation $\langle \gamma_N \rangle > \sigma_{\gamma}$ is satisfied and stable.

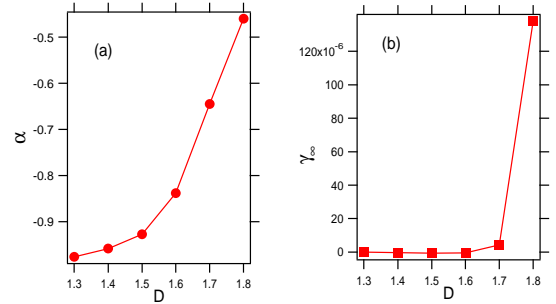


Fig. 12. (Color online) D -dependence of the fitting parameter (a) α and (b) γ_∞ in Eq.(7).

a metallic band of extended states in the finite region of the energy exists for $D \simeq 3/2$. In addition, the power-law localized states have been observed for $D \geq 3/2$, with decreasing the fractal dimension D in the cases. On the other hand, the N -dependence of the NLL suggests that for the strong disorder cases all the states are exponentially localized even for $1.3 < D \lesssim 1.5$, which is consistent with the finding of Ref.[27]. We have revealed the anomalous distribution of the individual NLL, as well as found that the asymptotic behaviour of the ensemble-average for Lyapunov exponent $\langle \gamma_N \rangle$ consists in that the latter goes to zero with increasing the system's size for $D \leq 1.7$.

The same properties as in the 1D electronic system given in this paper are also expected for the delocalization of acoustic wave [33,34,35], electromagnetic wave [36, 37] and seismic wave [38] in one-dimensional layered media with fractal disorder. We expect that the present work would stimulate further studies of the localization-delocalization transition in 1DDS.

A potential roughness and eigen functions

The LDT is closely connected to the relation between roughness of the potential landscapes and the degree of differentiability of the potential in the continuum limit

[39,23,24,25,26,40] It has been proposed that delocalized states can be generated for continuum 1DDS provided that the disorder potential is $V(x) \in C^\beta$ with $\beta > 1/2$ [23, 24]. The eigenstates are delocalized by properly changing the parameter L which controls the fluctuation of the potential. The singularity of the potential could be regulated by increasing the parameter L , as given in Fig.13.

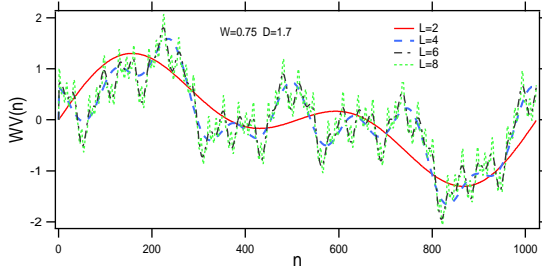


Fig. 13. (Color online) Typical on-site energy landscape $WV(n)$ generated by Eq.(2) with $L = 2, 4, 6, 8$ and $D = 1.7$. A case of $N = 2^{10}$ and $W = 0.75$ is shown. Notice that ones for $L > 10$ can not be distinguishable in this scale.

In Fig.14 the wavefunction absolute values for some eigenstates versus the site index are shown, using rigid boundary condition. It is found that the eigenstates closest to the center of the spectrum tend to be more delocalized than those closer to its edge. In particular, in the case of $L = 8$ the eigenstate close to center of the spectrum is localized even for $D = 1.7$ as shown in Fig.14(c).

Acknowledgments

The author would like to thank Professor M. Goda for discussion about the correlation-induced delocalization at early stage of this study and Professor E.B. Starikov for proof reading of the manuscript. The author also would like to acknowledge the hospitality of the Physics Division of The Nippon Dental University at Niigata for my stay, where part of this work was completed. The sole author had responsibility for all parts of the manuscript.

References

1. K. Ishii, Prog. Theor. Phys. Suppl. **53**, 77(1973).
2. E. Abrahams, P. W. Anderson, D. C. Licciardello, and T. V. Ramakrishnan, Rhys. Rev.Lett. **42**, 673 (1979).
3. L.M. Lifshiz, S.A. Gredeskul and L.A. Pastur, *Introduction to the theory of Disordered Systems*, (Wiley, New York,1988).
4. H. Yamada, M. Goda and Y. Aizawa, J. Phys.: Condens. Matter **3**, 10043(1991), H.Yamada, Phys. Rev. B **69** 014205(2004), H.Yamada, Phys. Lett. A **325** 118(2004), H. Yamada, H.Yamada and T.Okabe, Phys. Rev. E **63**, 026203(2001).
5. C.R. de Oliveira and G.Q. Pellegrino, J. Phys. A **34**, L239-L243 (2001).

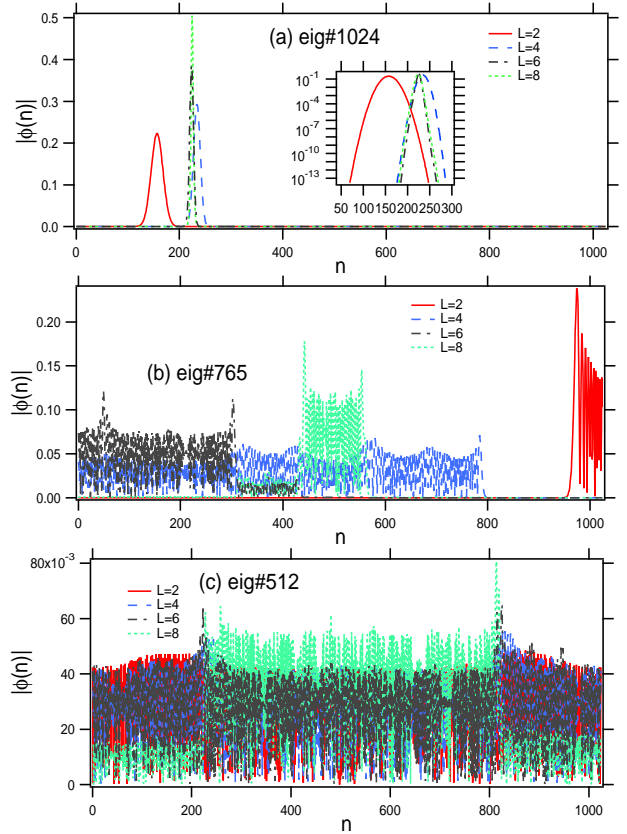


Fig. 14. (Color online) Comparison of some eigenstates $|\phi(n)|$ for the cases of $L = 2, 4, 6, 8$ in Fig.13 with $D = 1.7$ and $W = 0.75$. (a)The 1028th energy eigenstates closest to the spectrum edge, (b)the 768th energy eigenstates, (c)the 512th energy eigenstates closest to the spectrum center. Note that the horizontal axis in real scale. Inset of the panel (a) is the logarithmic plot.

6. R. A. Pinto, M. Rodriguez, J. A. Gonzalez, and E. Medina, Phys. Lett. A **341**, 101-106(2005).
7. A. Esmailpour, H. Cheraghchi, P. Carpena and M. R. R. Tabar, J. Stat. Mech. P09014(2007).
8. M. O. Sales, F. A. B. F. de Moura, Physica E **45**, 97-102(2012).
9. H. Cheraghchi, S. M. Fazeli, and K. Esfarjani, Phys. Rev. B **72**, 174207(2005).
10. E. Lazoa, E. Diezb, Phys. Lett. A **374**, 35383545(2010).
11. F.A.B.F.de Moura, and M.L.Lyra, Phys. Rev. Lett. **81** 3735(1998).
12. F.M.Izrailev and A.A.Krokhin, Phys. Rev. Lett. **82**, 4062(1999).
13. F. M. Izrailev, A. A. Krokhin, and N. M. Makarov, Phys. Rep. **512**, 125 (2012).
14. G.-P. Zhang and S.-J. Xionga, Eur. Phys. J. B **29**, 491-495(2002).
15. H.Shima, T.Nomura and T.Nakayama, Phys. Rev. B **70**, 075116(2004).
16. T. Kaya, Eur. Phys. J. B **55** (2007) 49.
17. T. Kaya, Eur. Phys. J. B **67** (2009) 225.
18. L.Y. Gong, P.Q. Tong, and Z.C. Zhou, Eur. Phys. J. B **77**, 413-417(2010).

19. A. Croy, P. Cain, and M. Schreiber, Eur. Phys. J. B **82**, 107 (2011).
20. Chao-Sheng Deng, and HuiXu, Physica E **44** 1473-1477(2012).
21. L. Gong, L. Wei, S. Zhao, and W. Cheng, Phys. Rev. E **86**, 061122 (2012).
22. C. Albrecht and S. Wimberger, Phys. Rev. B **85**, 045107 (2012).
23. A. M. Garcia-Garcia, and E. Cuevas, Phys. Rev. B **79**, 073104 (2009).
24. A. M. Garcia-Garcia, and E. Cuevas, Phys. Rev. B **82**, 033412 (2010).
25. G.M. Petersen and N. Sandler, arXiv:1206.3370v3 [cond-mat.dis-nn].
26. G.M. Petersen and N. Sandler, Phys. Rev. B **87**,195443(2013).
27. H.S. Yamada, Eur. Phys. J. B **88**, 264(2015).
28. P. Dean, Rev. Mod. Phys. **44**, 127(1972).
29. J. J. Ladik, *Quantum Theory of Polymers as Solids*. (Plenum Press, New Yourk, London 1988).
30. Shi-Jie Xiong and S. N. Evangelou, Phys. RevB. **64**.113107(2001).
31. Igor Travenec, physica status solidi b **245**, 1604(2008).
32. L. Bellando, A. Gero, E. Akkermans, and R. Kaiser, Phys. Rev. A **90**, 063822(2014).
33. Ayoub Esmailpour, M. Esmailpour, Ameneh Sheikhan, M. Elahi, M. Reza Rahimi Tabar, and Muhammad Sahimi, Phys. Rev. B **78**, 134206(2008).
34. A.E. Costa, and F.A.B.F. de Moura, J. Phys.: Condens Matter, **23**, 065101(2011).
35. M. P. S. Junior, M.L. Lyra and F. A. B. F. de Moura, Acta. Phys. Pol. B **46**, 1247(2015).
36. P. Sheng, *Scattering and Localization of Classical Waves in Random Media*, (World Scientific, Singapore, 1990).
37. E. Diaz, A. Rodriguez, F. Domnguez-Adame and V. A. Malyshev, Europhys. Lett. **72**, 1018-1024(2005).
38. F. Shahbazi, Alireza Bahraminasab, S. Mehdi Vaez Allaei, Muhammad Sahimi, and M. Reza Rahimi Tabar, Phys. Rev. Lett. **94**, 165505(2005).
39. N. P. Greis and H. S. Greenside, Phys. Rev. A **44**, 2324(1991).
40. H.S.Yamada and K.S. Ikeda, Eur. Phys. J. B **87**, 208(2014).